$[(MeTPP)Fe^{III}X]^+$ one pyrrole resonance is clearly distinct from the other three and shows a considerable upfield shift. Likewise in $[(MeOEP)Fe^{III}Cl]^+$ there are two methylene resonances (at 55 and 23 ppm) that are shifted upfield so that they are set apart from all others.

The logical conclusion that follows is that N-methylation primarily affects spin transfer to the modified pyrrole ring. This leads to sharply decreased shifts for both the pyrrole protons and methylene groups of that modified ring. The three "normal" pyrrole rings exhibit proton and methylene shift patterns that are similar to those found for symmetrical, five-coordinate, high-spin iron(III) porphyrins. The similarity of the two meso-proton shifts in $[(MeOEP)Fe^{III}Cl]^+$ to those of $(OEP)Fe^{III}Cl$ again indicates that the porphyrin molecular orbitals, particularly the π orbitals, are largely intact and that the difference in shift patterns between $(TPP)Fe^{III}Cl$ or $(OEP)Fe^{III}Cl$ and $[(MeTPP)Fe^{III}Cl]^+$ or $[(MeOEP)Fe^{III}Cl]^+$ originates primarily in sharply attenuated σ-spin transfer to the methylated pyrrole as a consequence of the longer Fe–N distance tilting of the pyrrole ring out of the porphyrin plane and change in nitrogen hybridization.

Experimental Section

Chloroform-*d* (Aldrich) was dried over 4-Å molecular sieves before use. Samples of the iron(II) porphyrins **6**–**10** and the deuterated derivatives were prepared by established procedures, which we described and acknowledged previously.[10]

Oxidation Procedures. Solutions of known concentrations (ca. 1 mM for NMR, 0.1 mM for electronic spectroscopy) of the iron(II) complexes **6**–**10** were prepared in chloroform-*d* and cooled to ~−50 °C in a dry ice/acetonitrile bath. Solutions of known concentrations of the halogen oxidant in chloroform were then transferred with a glass pipet into the cold sample of the iron(II) complex. Addition was performed slowly to minimize warming of the sample. The cold samples were then transferred to the appropriate spectrometer for measurements.

Instrumentation. NMR spectra were recorded on a Nicolet NT-360 FT spectrometer (for 360-MHz ^1H NMR spectra) or a Nicolet NT-500 FT spectrometer (for 76.7-MHz ^2H NMR spectra) operating in the quadrature mode. Between 200 and 1000 transients were accumulated over a 40-kHz bandwidth with 16K data points for ^1H NMR (4–8K for ^2H NMR) and a 6-μs 90° pulse. The signal-to-noise ratio was improved by apodization of the free-fraction decay, which introduced a negligible 3–10 Hz of line broadening. Line widths were determined for nonoverlapping peaks by using the Nicolet computer subroutine LF, which fit the peaks to a Lorentzian line. Overlapping peaks were fit with the NTCCAP routine. The line broadening introduced by apodization was subtracted from the line widths. The peaks were referenced against tetramethylsilane. Electronic spectra were measured with a Hewlett-Packard 8450 A spectrophotometer or with a Cary 17 spectrophotometer equipped with a Kontes low-temperature optical cell and Dewar. Electron spin resonance spectra were recorded on a Varian E3 spectrometer.

Acknowledgment. We thank the National Institutes of Health (Grant GM26226) for financial support. L.L.-G. was on leave from the Institute of Chemistry, University of Wroclaw, Wroclaw, Poland.

Registry No. **6**, 64813-94-1; **6**$^+$, 96760-81-5; **7**, 95675-69-7; **7**$^+$, 96760-82-6; **8**, 95675-71-1; **8**$^+$, 96760-83-7; **9**, 95675-73-3; **9**$^+$, 82057-14-5; **10**, 95675-74-4; **10**$^+$, 96791-12-7.

Contribution from the Department of Chemistry,
Montana State University, Bozeman, Montana 59717

Proton Transfer and Ligand Displacement Reactions of Nickel(II) *N,N'*-Bis(2-aminoethyl)oxaldiamide

KIM E. GILMORE and GORDON K. PAGENKOPF*

Received December 11, 1984

The transfer of Ni(II) from *N,N'*-bis(2-aminoethyl)oxaldiamide, $NiH_{-2}ODEN$, to triethylenetetramine proceeds through three general routes. One of these is a dissociative path, $k_{H_2O} = 0.001\ s^{-1}$. Another is a proton-dependent pathway that involves adding a proton, $K = 6.1 \times 10^6\ M^{-1}$, followed by dissociation, $k_2 = 0.035\ s^{-1}$, or reaction with another proton, $7.0 \times 10^3\ M^{-1}\ s^{-1}$. The third route involves the replacing ligand and provided steady-state rate constant ratios, $k_{HT}/k_T = 0.25$ and $k_{H_2T}/k_T = 0.18$. The steady-state formation constant was $0.7\ s^{-1}$. The mechanism observed for EDTA is similar except in the magnitude of the EDTA-dependent constants. The steady state formation constant is less, $0.038\ s^{-1}$, and the ratio for the species is $k_{H_2Y}/k_{HY} = 35$. When the first proton adds, it is believed to form a five-membered ring.

Complexation of nickel(II) by *N,N'*-bis(2-aminoethyl)oxaldiamide is similar in several coordination sites to that obtained by other polypeptide ligands. Sketch I of the complex demonstrates the orientation of the donors and the chelate rings.[1] All three of the chelate rings are five-membered, and the negative charge is concentrated on one side of the low-spin yellow complex. This complex is similar to several complexes through elemental composition of the chelate rings. For example, it is similar to $NiH_{-2}MBAE$ since both have the amide group in the interior chelate ring.[2] It is also similar to $NiH_{-2}DGEN$ by having terminal coordination[3] of $-NH_2$.

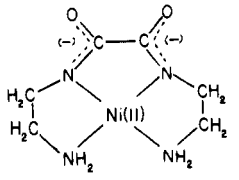

I, $NiH_{-2}ODEN$

This complex was reacted with triethylenetetramine and ethylenediaminetetraacetate over a sizable pH range. Similar reactions have studied the transfer of nickel(II) from triglycine,[4,5] diglycylamide,[6] tetraglycine,[7] and glycylglycylhistidine.[8] The reactions of $NiH_{-2}ODEN$ with the two displacing ligands proceed through a variety of parallel paths that may include protonated intermediates.

Experimental Section

The nickel stock solution, 0.100 M, was prepared from twice recrystallized $Ni(ClO_4)_2$ and was standardized by EDTA titration. Twice recrystallized $NaClO_4$ was used to maintain the ionic strength at 0.10 M for the kinetic runs. The trien stock solution was prepared from the twice recrystallized sulfate salt and standardized spectrophotometrically (575 nm) with use of standard copper(II). Primary standard Na_2EDTA was utilized. The ODEN ligand was synthesized by the Hill and Raspin method.[1] The nickel–ODEN complexes were prepared just before the

(1) Hill, H. A. O.; Raspin, K. A. *J. Chem. Soc. A* **1968**, 3036.
(2) Storvick, J. P.; Pagenkopf, G. K., submitted for publication in *Inorg. Chem.* 1984.
(3) Storvick. J. P.; Pagenkopf, G. K. *Inorg. Chem.*, in press.
(4) Bannister, C. E.; Margerum, D. W. *Inorg. Chem.* **1981**, *20*, 3149.
(5) Brice, V. T.; Pagenkopf, G. K. *J. Chem. Soc., Chem. Commun.* **1974**, *75*.
(6) Mason, C. F. V.; Chamberlain, P. I.; Wilkins, R. G. *Inorg. Chem.* **1971**, *10*, 2345.
(7) Paniago, E. B.; Margerum, D. W. *J. Am. Chem. Soc.* **1972**, *94*, 6704.
(8) Bannister, C. E.; Raycheba, J. M. T.; Margerum, D. W. *Inorg. Chem.* **1982**, *21*, 1106.

0020-1669/85/1324-2436$01.50/0

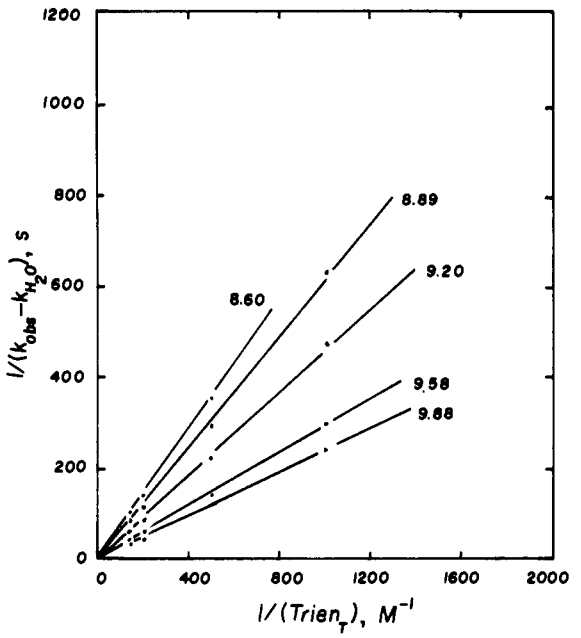

Figure 1. [trien$_T$] dependence of observed rate constant at pH greater than 8.5.

kinetic measurements. There was 50% excess ligand added, and the initial pH was always less than 5. The solutions were bubbled with nitrogen prior to and during a slow pH increase to 9 or above. If oxygen was not removed and kept out, there would be a major change in the nature of the nickel–ODEN complex. The reactions usually had a total nickel concentration of 5.0×10^{-4} M.

No buffer was added to the complex solution for the reactions below pH 9. For the ones above pH 9, 0.005 M borate was utilized. The pH range 7.4–8.8 was maintained by 0.01 M tris(hydroxymethyl)aminomethane (Tris), 2-picoline, 0.01 M, was used for the pH range 5.5–7.1 and 0.01 M acetate buffer was utilized for the pH range 4.5–5.0. These buffers were only present in the trien or EDTA solutions prior to mixing.

The slow reactions were monitored by the Varian 634 spectrophotometer. The molar absorptivities of NiH$_{-2}$ODEN are 187 M^{-1} cm^{-1} at 414 nm and 2980 M^{-1} cm^{-1} at 307 nm. Most of the reactions were monitored in the UV region. The rapid reactions used a Durrum 103 stopped-flow spectrophotometer. The temperature was 25.0 °C, and hydrogen ion concentration was obtained from $-\log [H^+] = pH - 0.10$. The reactions were always run at least in triplicate, and the subsequently listed rate constant values are averages. The computer program "LLJAC"[9] was used where appropriate. Under pseudo-first-order conditions the plots of ln $(A_t - A_\infty)$ vs. time are linear for at least 3–4 half-lives.

Results

Reaction of NiH$_{-2}$ODEN with trien, pH >8.5. The reaction of NiH$_{-2}$ODEN with trien$_T$ under pseudo-first-order conditions provides rate constants that are dependent upon the pH and the trien$_T$ concentration. These rate constants are not precisely dependent upon trien$_T$, however. Analysis of the data indicates that parallel paths are occurring (eq 1–3). A steady-state treatment

$$\text{NiH}_{-2}\text{ODEN} + \text{H}_2\text{O} \rightarrow \text{product} \quad (1)$$

$$\text{NiH}_{-2}\text{ODEN} \underset{k_{-1}}{\overset{k_1}{\rightleftharpoons}} \text{Ni}^* \quad (2)$$

$$\text{Ni}^* + \text{trien}_T \xrightarrow{k_{TT}} \text{product} \quad (3)$$

for Ni* provides the effective rate expression in this pH range, and it is shown in eq 4.

$$\text{rate} = \left(k_{H_2O} + \frac{k_1 k_{TT}[\text{trien}_T]}{k_{-1} + k_{TT}[\text{trien}_T]} \right)[\text{Ni}_T] \quad (4)$$

(9) Howald, R. A. "LLJAC Program", Montana State University, private communication, 1983.
(10) Billo, E. J.; Smith, G. F.; Margerum, D. W. *J. Am. Chem. Soc.* **1971**, *93*, 2635.
(11) Raycheba, J. M. T.; Margerum, D. W. *Inorg. Chem.* **1980**, *19*, 837.
(12) Raycheba, J. M. T.; Margerum, D. W. *Inorg. Chem.* **1980**, *19*, 497.

Table I. Kinetic Data for the Reaction of NiH$_{-2}$ODEN with trien$_T$

10^3[trien$_T$], M	k_{obsd}, s^{-1}	pH	10^3[trien$_T$], M	k_{obsd}, s^{-1}	pH
1.0	0.00479	9.88	1.0	0.0250	6.65
2.0	0.0090	9.88	2.0	0.0236	6.60
5.0	0.0218	9.88	5.0	0.0267	6.54
7.0	0.0304	9.88	7.0	0.0282	6.50
1.0	0.00407	9.58	1.0	0.0289	6.22
2.0	0.00781	9.58	2.0	0.030	6.21
5.0	0.017	9.58	5.0	0.0309	6.16
7.0	0.0245	9.58	7.0	0.0324	6.15
1.0	0.00293	9.20	1.0	0.0353	5.94
2.0	0.0053	9.20	2.0	0.0367	5.92
5.0	0.0123	9.20	5.0	0.0371	5.92
7.0	0.0162	9.20	7.0	0.0369	5.88
1.0	0.00255	8.89	1.0	0.0433	5.73
2.0	0.00434	8.89	2.0	0.0442	5.70
5.0	0.0094	8.89	5.0	0.0458	5.68
7.0	0.0124	8.89	7.0	0.0463	5.66
1.0	0.00221	8.60	1.0	0.060	5.41
2.0	0.00401	8.60	2.0	0.0586	5.47
5.0	0.00823	8.60	5.0	0.0591	5.43
7.0	0.0108	8.60	7.0	0.0643	5.39
1.0	0.00418	8.11	1.0	0.0840	5.09
2.0	0.00568	8.09	2.0	0.0879	5.06
5.0	0.0100	8.03	5.0	0.100	4.97
7.0	0.0119	8.01	7.0	0.111	4.93
1.0	0.00721	7.73	1.0	0.128	4.85
2.0	0.0091	7.72	2.0	0.136	4.86
5.0	0.0138	7.66	5.0	0.159	4.78
7.0	0.0161	7.64	7.0	0.173	4.75
1.0	0.0092	7.46	1.0	0.216	4.58
2.0	0.0117	7.42	2.0	0.211	4.56
5.0	0.0161	7.37	5.0	0.262	4.49
7.0	0.0188	7.30	7.0	0.301	4.46

Since the observed rate constants are equal to the components in parentheses, rearrangement provides the expression

$$\frac{1}{k_{obsd} - k_{H_2O}} = \frac{1}{k_1} + \frac{k_{-1}}{k_1 k_{TT}[\text{trien}_T]} \quad (5)$$

The best fit to the data is obtained when $k_{H_2O} = 0.001$ s^{-1}. With use of this value, linear plots of $1/(k_{obsd} - k_{H_2O})$ vs. $1/[\text{trien}_T]$ are obtained as evidenced in Figure 1. The figure intercept provides a value of $k_1 = 0.7 \pm 0.3$ s^{-1}. Slopes provide values for k_{-1}/k_{TT}, and by using the α values of the trien species at the different pH values, one can calculate the ratios of the trien species rate constants. They are $k_{HT}/k_T = 0.25$ and $k_{H_2T}/k_T = 0.18$. The data are summarized in Table I.

Reaction of NiH$_{-2}$ODEN with trien, pH <8.5. As the pH of the reaction mixture decreases, the trien$_T$ dependence decreases, and ultimately there is minimal contribution from the trien pathway. For example, at pH 5.7 the increase in k_{obsd} as trien$_T$ varies is similar to experimental uncertainty. This is because most of the reaction proceeds through a proton-dependent pathway. A second-order hydrogen ion dependence is approached in the pH 6 region; however, it decreases to first order by the pH 5 region (see eq 6–8). The observed rate constant for the trien$_T$-independent pathways is shown in eq 9.

$$\text{NiH}_{-2}\text{ODEN} + \text{H}_3\text{O}^+ \underset{}{\overset{K_H}{\rightleftharpoons}} \text{NiH}_{-2}\text{ODEN}\cdot\text{H}^+ + \text{H}_2\text{O} \quad (6)$$

$$\text{NiH}_{-2}\text{ODEN}\cdot\text{H}^+ \xrightarrow{k_2} \text{product} \quad (7)$$

$$\text{NiH}_{-2}\text{ODEN}\cdot\text{H}^+ + \text{H}_3\text{O}^+ \xrightarrow{k_{H_3O}} \text{product} \quad (8)$$

$$k_i - k_{H_2O} = (k_2 + k_{H_3O}[\text{H}_3\text{O}^+])\frac{K_H[\text{H}_3\text{O}^+]}{1 + K_H[\text{H}_3\text{O}^+]} \quad (9)$$

The k_i values are equal to the intercepts of the plots of k_{obsd} vs. trien$_T$. A plot of $k_i - k_{H_2O}$ vs. $[H_3O^+]$ is shown in Figure 2. The slope portion provides k_{H_3O}: $k_{H_3O} = 7.0 \times 10^3$ M^{-1} s^{-1}, and extrapolation to zero H_3O^+ provides $k_2 = 0.035$ s^{-1}. The data at H_3O^+ concentration less than 3×10^{-6} M (pH 5.5) were utilized to calculate K_H: $K_H = 6.1 \times 10^6$ M^{-1}. It has been assumed that

Table II. Kinetic Data for the Reaction of $NiH_{-2}ODEN$ with $EDTA_T$

10^3[EDTA], M	k_{obsd}, s^{-1}	pH	10^3[EDTA], M	k_{obsd}, s^{-1}	pH
1.0	0.00100	9.96	7.0	0.0220	7.54
2.0	0.00153	9.96	7.0	0.0250	7.55
5.0	0.00315	9.95	2.0	0.0260	6.64
7.0	0.00475	9.93	5.0	0.0283	6.59
1.0	0.00199	9.48	7.0	0.0286	6.57
2.0	0.00304	9.49	1.0	0.0329	6.27
5.0	0.00643	9.47	2.0	0.0323	6.28
7.0	0.0087	9.44	5.0	0.0333	6.25
1.0	0.00407	8.91	7.0	0.0346	6.23
2.0	0.00582	8.91	1.0	0.0348	6.00
5.0	0.0103	8.91	2.0	0.0357	5.98
7.0	0.0118	8.92	5.0	0.0386	5.96
1.0	0.00550	8.51	7.0	0.0382	5.95
2.0	0.0080	8.51	1.0	0.0436	5.78
5.0	0.0141	8.49	2.0	0.0429	5.77
7.0	0.0165	8.46	5.0	0.0443	5.75
7.0	0.0172	8.51	7.0	0.0447	5.73
1.0	0.0103	7.88	1.0	0.0523	5.52
2.0	0.0142	7.87	2.0	0.0541	5.49
5.0	0.0199	7.85	5.0	0.0564	5.47
7.0	0.0232	7.82	7.0	0.057	5.46
7.0	0.0240	7.82	1.0	0.128	4.88
1.0	0.0130	7.59	2.0	0.127	4.87
2.0	0.0162	7.58	5.0	0.134	4.86
5.0	0.0210	7.57	7.0	0.144	4.84

Table III. Rate Constants for the Reactions of trien and EDTA with $NiH_{-2}ODEN$

const	value
k_{H_2O}	0.0010 ± 0.0006 s^{-1}
k_1	0.7 ± 0.3 s^{-1}
k_4	0.038 ± 0.005 s^{-1}
k_2(trien reacn)	0.035 ± 0.002 s^{-1}
k_2(EDTA reacn)	0.033 ± 0.002 s^{-1}
k_{H_3O}(trien reacn)	$(7.0 \pm 0.4) \times 10^3$ M^{-1} s^{-1}
k_{H_3O}(EDTA reacn)	$(6.7 \pm 0.4) \times 10^3$ M^{-1} s^{-1}
K_H	$(6.1 \pm 0.3) \times 10^6$ M^{-1}
k_{HT}/k_T	0.25
k_{H_2T}/k_T	0.18
k_{H_2Y}/k_{HY}	35
k_{-1}/k_T	0.12
k_{-4}/k_{HY}	0.025

the species Ni* does not increase in concentration, thus negating the steady-state treatment. Combination of the $trien_T$-dependent and -independent pathways permits prediction of the observed rate constant—one example is shown in Figure 3. The data are included in Table I.

Reaction of $NiH_{-2}ODEN$ with EDTA. The reaction of the nickel–ODEN complex with EDTA at pH values less than 7 proceeded the same way as was observed for the reaction with $trien_T$. This is shown by eq 6–9. The rate constants for the EDTA reactions are $k_2 = 0.033$ s^{-1} and $k_{H_3O} = 6.7 \times 10^3$ M^{-1} s^{-1}. Utilization of the same value for K_H (6.1×10^6 M^{-1}) provides good agreement between the observed and predicted rate constants. In this pH range EDTA is not competitive with H_3O^+.

In the higher pH range 7.57–9.96 the reactive pattern is similar to that observed in the $trien_T$ reactions, but it is not exactly the same as evidenced by the magnitude of the observed rate constants. The path shown in eq 1 is present, and it is combined with another steady-state consideration:

$$NiH_{-2}ODEN \underset{k_{-4}}{\overset{k_4}{\rightleftharpoons}} \quad (10)$$

$$Ni^{**} + EDTA_T \xrightarrow{k_{YT}} \text{products} \quad (11)$$

The observed rate constant is equal to

$$k_{obsd} = k_{H_2O} + \frac{k_4 k_{YT}[EDTA_T]}{k_{-4} + k_{YT}[EDTA_T]} \quad (12)$$

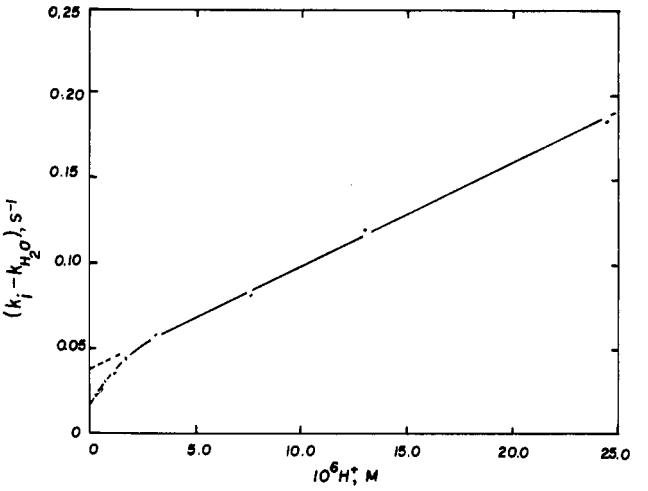

Figure 2. Dependence of observed rate constant on $[H_3O^+]$ in the low-pH range.

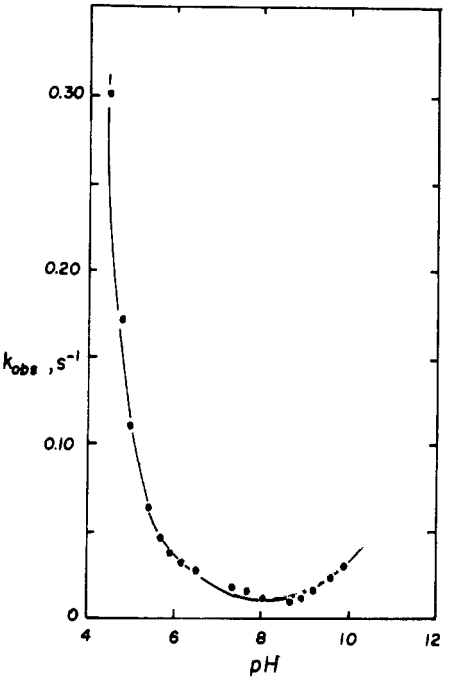

Figure 3. Predicted pH profile for the reaction of $NiH_{-2}ODEN$ with trien, $[trien_T] = 7.0 \times 10^{-3}$ M.

Table IV. Constants for Nickel(II) Polypeptide Complexes

complex	log K_H, M^{-1}	k_2, s^{-1}	ref
$NiH_{-2}ODEN{\cdot}H$	6.79	0.035	this work
$NiH_{-2}GGHis{\cdot}H$	4.3	1.5	8
$NiH_{-3}G_4{\cdot}H$	4.25	5.6	7
$NiH_{-3}G_4a{\cdot}H$	2.4	12	12

A plot of $1/(k_{obsd} - k_{H_2O})$ vs. $1/[EDTA_T]$ for the various pH values is shown in Figure 4. The value of k_4 is 0.038 s^{-1}. The ratio of the EDTA species is $k_{H_2Y}/k_{HY} = 35$. The EDTA replacement data are listed in Table II. All of the rate constants, the equilibrium constant, and the rate constant ratios are listed in Table III.

Discussion

Reaction with $trien_T$. Trien has reacted with a variety of both nickel and copper polypeptide complexes. In general, the reaction rate is greatest with the copper complexes,[13,14] but the rate can dramatically drop when glycine is replaced by histidine.[15] The

(13) Pagenkopf, G. K.; Margerum, D. W. *J. Am. Chem. Soc.* **1968**, *90*, 502.
(14) Pagenkopf, G. K.; Margerum, D. W. *J. Am. Chem. Soc.* **1970**, *92*, 2683.

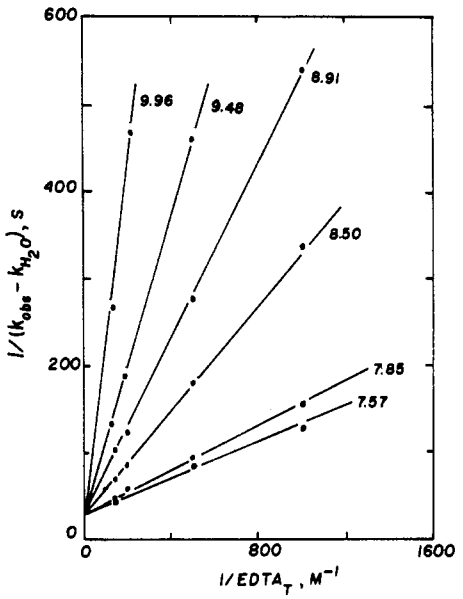

Figure 4. Dependence of k_{obsd} upon total EDTA concentration in the higher pH range.

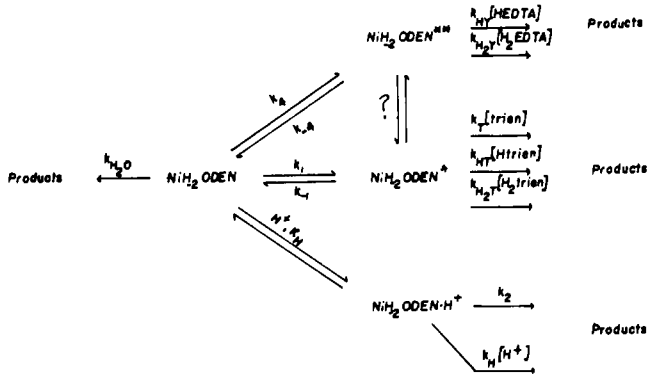

Figure 5. Reaction pathways for the transfer of Ni(II) from $NiH_{-2}ODEN$ in the presence of trien and EDTA.

ligand used in this work, ODEN, is similar to the polypeptide complexes in that it has four donors and forms a square-planar complex. There are some structural differences between $NiH_{-2}ODEN$ and polypeptide complexes, however. The two most significant differences are the terminal amine donors and the fact that both deprotonated amide groups are in one chelate ring. These results provide an indication of how configuration rearrangement alters the kinetic properties. The reaction rate for $trien_T$ with $NiH_{-2}ODEN$ is less than what is observed for the reaction with the triglycine complex,[10] $NiH_{-2}GGG^-$, but is larger than what has been observed for the glycylglycyl-*l*-histidine complex.[8]

The general reaction sequence is shown in Figure 5. The rate constant for the reaction with water equals 0.001 s^{-1}. This value is considerably less than that observed for triglycine, 0.088 s^{-1}, but is at least a factor of 10 greater than what has been observed for $NiH_{-2}GGHis^-$, $NiH_{-3}G_4^{2-}$, and $NiH_{-3}G_4a^-$.[7,8,12] The reaction routes with water are very difficult to identify, and thus minimal comments can be made.

The $trien_T$-dependent pathway for $NiH_{-2}ODEN$ exhibits kinetics different from what has been observed for other systems. In the other systems the value of k_{-1} is larger than $k_{TT}[trien_T]$, and thus there is preequilibrium prior to the rate-determining step. In this case the species designated as Ni* is believed to have one of the terminal amine groups of $NiH_{-2}ODEN$ not coordinated. This would provide a planar nickel coordination site for $trien_T$. Apparently recoordination of one of ODEN's terminal $-NH_2$ groups is slower, and thus the reaction profile shifts from preequilibrium to a steady state. The ratios of the trien species rate constants indicate that free trien is 4–5 times more reactive than $Htrien^+$ and H_2trien^{2+}. There is no indication of general-acid dependence, and thus the k_{H_2T} value is larger than what would be expected.

Proton Dependence. The proton dependence involves the formation of $NiH_{-2}ODEN \cdot H^+$, which is believed to have the configuration designated in II.

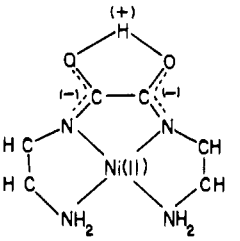

II, $NiH_{-2}ODEN \cdot H^+$

The added proton is bonded to both of the oxygen atoms, forming a five-membered ring. The value of the stability constant K_H is 6.1×10^6 M^{-1}. This constant is considerably larger than what has been observed for other complexes. For example, $NiH_{-2}GGHis^-$ exhibits a value of $10^{4.3}$. The constant[7] for $NiH_{-3}GGGG^{2-}$ is $10^{4.25}$, and a value for the tetraglycine amide[12] complex, $NiH_{-3}G_4a^-$, is $10^{2.4}$.

The positions of amide groups in the other complexes are such that the addition of a proton can only be associated with one oxygen. As shown in structure II, this is not the case for the ODEN complex. As a consequence, the stability of the complex is significantly increased.

Subsequent decomposition of this intermediate proceeds through two pathways. One of those is proton dependent and the other is proton independent. The magnitude of the rate constant for the proton-independent pathway is small and, again, reflects the kinetic stability added to the complex when a proton is bonded to the oxygens. The values for the rate constants are listed in Table IV. The largest difference, which is a factor of more than 300, lies between $NiH_{-3}G_4 \cdot H$ and $NiH_{-2}ODEN \cdot H^+$.

The other pathway involves the reaction with another proton. This sequence would involve disruption of the five-membered ring formed when the first proton added. Correspondingly, this should provide a rate constant that would be more similar to those observed for the other complexes. This is observed in at least one case. The k_{H_3O} rate constant for $NiH_{-2}GGHis^-$ is $10^{3.7}$ M^{-1} s^{-1}, which is very similar to the value of $10^{3.8}$ M^{-1} s^{-1} observed in this study.

Reaction with $EDTA_T$. The reaction of $NiH_{-2}ODEN$ with $EDTA_T$ is similar to that observed for the $trien_T$ reaction with one major exception (Figure 5). As evidenced, the reaction with water and the reaction with the proton are the same. The values of these rate constants are the same within the experimental uncertainty (Table III). This is expected since there is no replacing ligand dependence in these pathways.

The difference lies in the magnitude of k_4 and k_2 and possibly in the second-order rate constants, k_{YT} and k_{TT}. In general, EDTA is often sterically restricted in its nucleophilic reactivity and consequently reacts slower than trien. That cannot be resolved in this system since k_{-2}, k_{TT}, k_{-4}, and k_{YT} cannot be resolved. There is an indication that the same reactive pattern is operative here, though, by comparison of the values of k_2 and k_4. In this case the EDTA constant is a factor of 18 smaller and indicates that more of the original complex needs to dissociate before EDTA can react. The nature of this dissociation is not known, but it is possible that it proceeds along the pathway that is successful for trien. However, in the case of the EDTA, additional dissociation must occur. It is possible that the the reactive intermediate for the $trien_T$ pathway is the first step in the EDTA reaction.

Registry No. I, 20102-46-9; trien, 112-24-3; EDTA, 60-00-4.

(15) Wong, L. F.; Cooper, J. C.; Margerum, D. W. *J. Am. Chem. Soc.* **1976**, *98*, 7268.